

Regulation of MBK-2/Dyrk Kinase by Dynamic Cortical Anchoring during the Oocyte-to-Zygote Transition

Michael L. Stitzel,^{1,2} Ken Chih-Chien Cheng,^{1,2} and Geraldine Seydoux^{1,*}

¹Department of Molecular Biology and Genetics
Howard Hughes Medical Institute
Center for Cell Dynamics
Johns Hopkins School of Medicine
725 North Wolfe Street
PCTB 706
Baltimore, Maryland 21205

Summary

Background: Successful transition from oocyte to zygote depends on the timely degradation of oocyte proteins to prepare for embryonic development. In *C. elegans*, degradation of the oocyte protein MEI-1 depends on MBK-2, a kinase that phosphorylates MEI-1 shortly after fertilization during the second meiotic division.

Results: Here we report that precise timing of MEI-1 phosphorylation depends on the cell cycle-regulated release of MBK-2 from the cortex. Prior to the meiotic divisions, MBK-2 is tethered at the cortex by EGG-3, an oocyte protein required for egg activation (see [1], accompanying paper in this issue). During the meiotic divisions, EGG-3 is internalized and degraded in an APC/C (anaphase-promoting complex/cyclosome)-dependent manner. EGG-3 internalization and degradation correlate with MBK-2 release from the cortex and MEI-1 phosphorylation in the cytoplasm. In an *egg-3* mutant, MEI-1 is phosphorylated and degraded prematurely.

Conclusion: We suggest that successful transition from an oocyte to a zygote depends on the cell cycle-regulated relocalization of key regulators from the cortex to the cytoplasm of the egg.

Introduction

In most animals, reproduction depends on fusion of an oocyte with sperm to form a fertilized egg or zygote. Progression from oocyte to zygote can be divided into two phases: oocyte maturation and egg activation [2]. During maturation, fully-grown oocytes, arrested at the end of prophase of meiosis I, are stimulated by extracellular signals to reenter meiotic M phase and initiate the meiotic divisions. Oocytes typically are ovulated during that time and reach a second meiotic arrest point awaiting fertilization [3]. Egg activation—in many species triggered by sperm entry—stimulates the mature egg to complete the meiotic divisions, form pronuclei, and initiate mitosis [4]. Whereas egg activation traditionally has been viewed as the critical step signaling the beginning of development, accumulating evidence suggests that oocyte maturation also sets in motion changes required

for successful transition to embryogenesis [2]. In mouse oocytes, maturation triggers reorganization of the endoplasmic reticulum and degradation of many RNAs associated with oocyte fate [5, 6]. In *C. elegans*, maturation activates the turnover of oocyte proteins that, if allowed to persist in the zygote, would interfere with embryogenesis [7]. Maturation also stimulates phosphorylation of RNA polymerase II, suggesting a possible role in transcriptional reactivation [8]. A major challenge is to understand how these changes are activated and coordinated with the meiotic divisions.

C. elegans oocyte maturation is stimulated by a sperm-secreted factor that signals the oocyte closest to the spermatheca to initiate the first meiotic division [9]. The mature oocyte is ovulated into the spermatheca, fertilized, and pushed out into the uterus where it completes the meiotic divisions and secretes an egg shell. Oocytes that undergo maturation, but are not fertilized, complete anaphase I but do not undergo the second meiotic division, form polar bodies, or secrete an egg shell [10]. These oocytes, however, still activate the degradation of oocyte proteins (e.g., MEI-1 and OMA-1) that need to be degraded for a smooth transition to embryonic development [7]. Degradation of MEI-1 and OMA-1 depends on MBK-2 [11–13]. MBK-2 belongs to the family of dual specificity YAK-related kinases (DYRK) [14]. MBK-2 phosphorylates MEI-1 and OMA-1 directly beginning in the second meiotic division, triggering their degradation in zygotes [7, 15, 16]. The mechanisms that specify the timing of MEI-1 and OMA-1 phosphorylation by MBK-2 are not known. Fertilization is not required, but progression through the first meiotic division is essential and sufficient, suggesting a link between meiotic progression and MBK-2 activation [7]. A GFP:MBK-2 fusion relocalizes from the egg cortex to the cytoplasm after meiosis I, raising the possibility that cell cycle-dependent internalization of MBK-2 is the critical trigger [7]. In the present study, we provide support for this hypothesis by identifying and characterizing EGG-3, an oocyte protein essential for MBK-2 localization to the cortex.

Results

EGG-3 Is Required for MBK-2 Localization to the Egg Cortex

We identified *F44F4.2* in an RNAi screen for genes required for MBK-2 localization to the cortex (Figure 1 and Experimental Procedures). *F44F4.2* was identified independently in a screen for genes required for egg activation and named *egg-3* (see [1], accompanying paper in this issue). A GFP:EGG-3 fusion localizes in a pattern similar to that reported for GFP:MBK-2 ([1], accompanying paper; and Figure 1). Like GFP:MBK-2, GFP:EGG-3 is enriched on the cortex of oocytes and newly fertilized zygotes. In anaphase of meiosis I, GFP:EGG-3 localizes to discrete subcortical puncta, which become internalized during the second meiotic division. GFP:EGG-3 is

*Correspondence: gseydoux@jhmi.edu

²These authors contributed equally to this work.

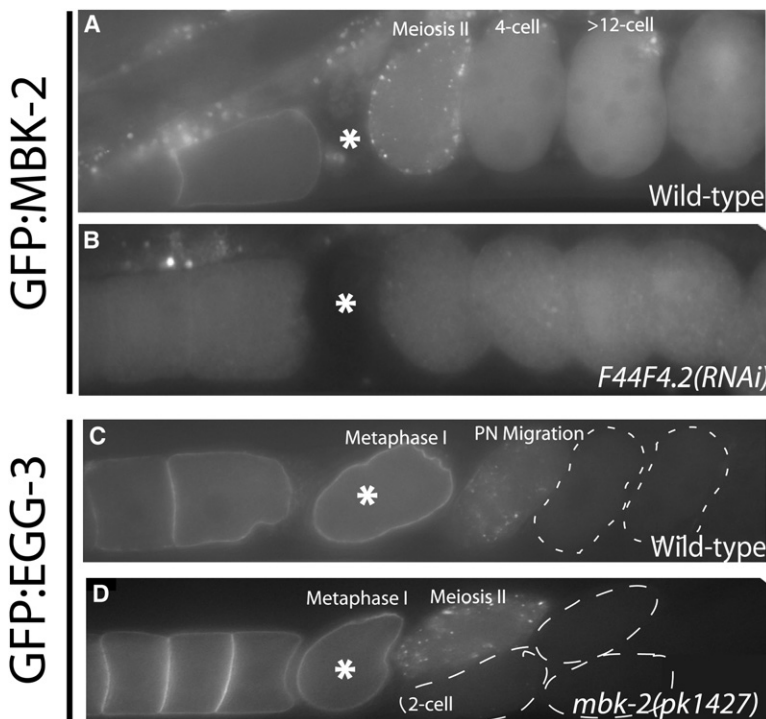


Figure 1. EGG-3 Is Required to Localize GFP:MBK-2 to the Cortex

(A and B) Live wild-type (A) and *egg-3[F44F4.2](RNAi)* (B) hermaphrodites expressing GFP:MBK-2. Each figure shows a close-up of the oviduct and uterus separated by the spermatheca (asterisk). Oocytes (left) and fertilized eggs (right) flank the spermatheca. Punctate gut autofluorescence is visible above the oocytes.

(C and D) Live wild-type (C) or *mbk-2(pk1427)* (D) hermaphrodites expressing GFP:EGG-3. Embryos lacking GFP:EGG-3 are outlined. Note that localization and turnover of GFP:EGG-3 in zygotes do not require *mbk-2*.

degraded after the 2-cell stage, unlike GFP:MBK-2, which remains present in the cytoplasm of all early blastomeres (Figure 1).

To visualize EGG-3 and MBK-2 directly, we generated antibodies to each protein (Experimental Procedures). As predicted from the GFP fusions, we found that endogenous MBK-2 and EGG-3 colocalize on the cortex of growing oocytes (Figure 2A). The antibody that we generated against MBK-2 recognizes MBK-2 only weakly during the meiotic divisions (Figure S1B in the Supplemental Data available online), preventing direct colocalization studies in these stages. We found, however, that two MBK-2 fusions (GFP:MBK-2 and MBK-2:His) colocalize with endogenous EGG-3 on the cortex in metaphase I embryos (Figure 2B; Figure S1C) and in discrete cytoplasmic puncta during the second meiotic division (Figure 2C; Figure S1C). In 2-cell and later embryos, EGG-3 was rarely detected, whereas GFP:MBK-2 (Figure 1) and endogenous MBK-2 (Figure S1B and data not shown) persisted in the cytoplasm of all blastomeres and on P granules until at least the 20-cell stage. Comparison of total EGG-3 levels to cytoplasmic GFP:MBK-2 levels confirmed that degradation of EGG-3 correlates with increased GFP:MBK-2 in the cytoplasm (Figure 2E).

We also examined MBK-2 and EGG-3 localizations in mutants homozygous for deletions in the *egg-3* or *mbk-2* genes (Experimental Procedures). In the *egg-3* deletion mutant *tm1191*, MBK-2 was cytoplasmic at all stages (Figure S1A). In contrast, in the *mbk-2* deletion mutant *pk1427* [11], EGG-3 remained cortical in oocytes, localized to internal puncta during meiosis, and disappeared after the 2-cell stage as in wild-type (Figures S1A and S1B). We conclude that, although MBK-2 depends on EGG-3 for cortical localization, EGG-3 does not depend on MBK-2 for its localization or turnover.

EGG-3 and MBK-2 Form a Complex In Vivo and In Vitro

EGG-3 encodes a putative protein tyrosine phosphatase (PTP) that is missing critical catalytic residues in its predicted active site (see Discussion), suggesting a possible function as an “antiphosphatase” or scaffold [17, 18]. To test whether EGG-3 and MBK-2 interact in vivo, we immunoprecipitated each protein from worm extracts. We detected EGG-3 in MBK-2 immunoprecipitates and MBK-2 in EGG-3 immunoprecipitates (Figures 3A and 3B). EGG-3 immunoprecipitates did not contain PAR-5 (Figure 3A), an abundant, cortically enriched protein [19], confirming that the EGG-3:MBK-2 interaction is specific. GFP antibodies could immunoprecipitate MBK-2 in extracts from worms expressing GFP:EGG-3 but not in extracts from worms expressing GFP alone (Figure 3C). We conclude that EGG-3 and MBK-2 form a complex in vivo.

To test whether the EGG-3:MBK-2 interaction is direct, we expressed both proteins as GST and FLAG fusions in *E. coli*. We found that GST:EGG-3-coupled beads could pull down FLAG:MBK-2 from *E. coli* extracts and, conversely, that GST:MBK-2 could pull down FLAG:EGG-3 (Figure 3D). GST alone interacted with neither FLAG fusions, confirming the specificity of the assay (Figure 3D). We conclude that EGG-3 and MBK-2 interact directly in vitro.

MEI-1 Is Phosphorylated and Degraded Prematurely in the Absence of EGG-3

To investigate the effect of EGG-3 on MBK-2 activity in vivo, we monitored MBK-2 activity with an antibody specific for MEI-1 phosphorylated on serine 92 (MEI-1-Ser92P), the site of MBK-2 phosphorylation [7]. To maximize MEI-1-Ser92P levels, we depleted by RNAi *mel-26*, the E3 ligase subunit that targets MEI-1 for degradation

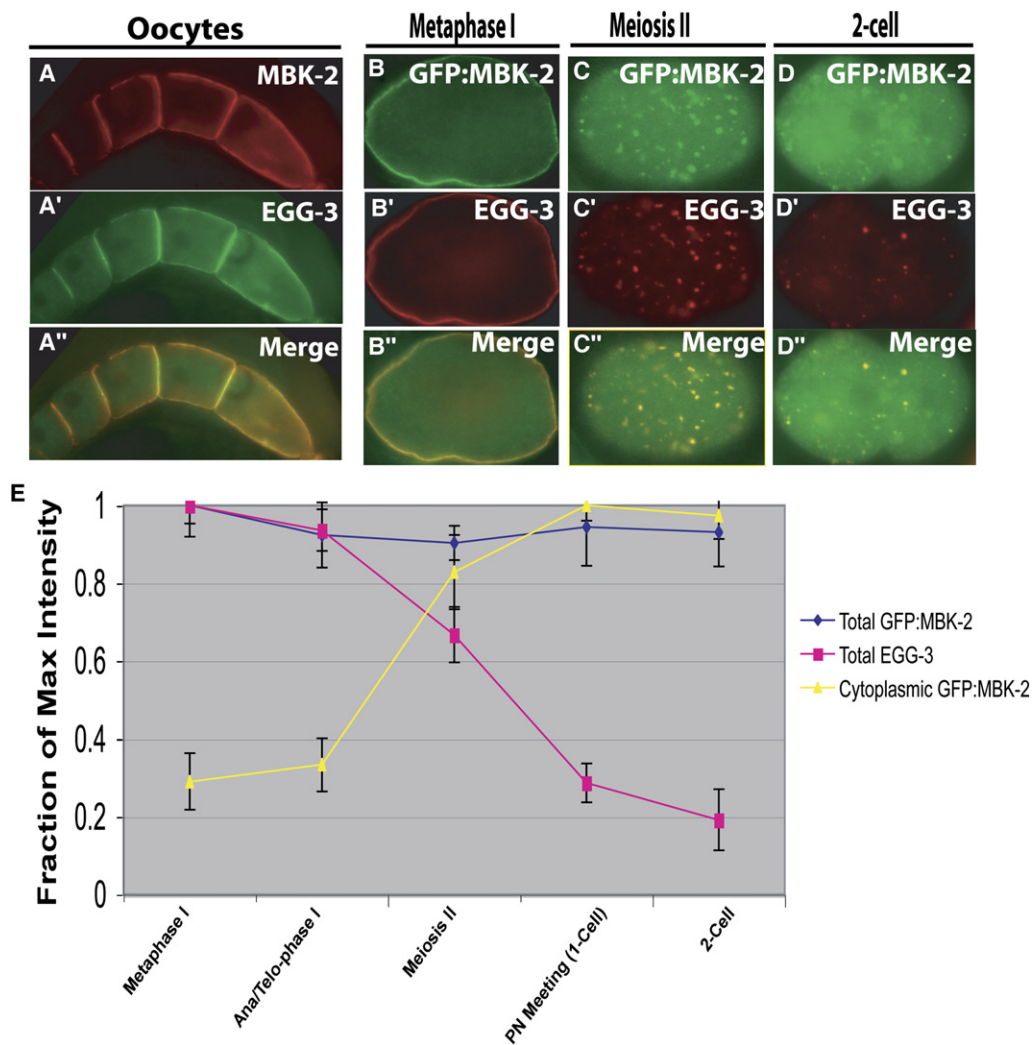


Figure 2. MBK-2 and EGG-3 Colocalize In Vivo

(A) Oocytes costained with α -MBK-2 (A) and α -EGG-3 (A') antibodies. Yellow indicates colocalization in the merged panel (A'').

(B–D) Embryos expressing GFP:MBK-2 costained with α -GFP (B–D) and α -EGG-3 (B'–D'). Yellow indicates colocalization in the merged panels (B''–D'').

(E) Graph showing relative levels of EGG-3 and GFP:MBK-2 at different stages. Error bars represent standard deviation.

[20]. As in wild-type, in *mel-26(RNAi)*, low levels of MEI-1-Ser92P are first detected in the cytoplasm during meiosis II and reach maximal levels after meiosis (Figure 4A). In contrast, in *egg-3(tm1191);mel-26(RNAi)*, high levels of MEI-1-Ser92P could be detected as early as metaphase of meiosis I. Prominent staining was detected both in the cytoplasm (6/7 eggs) and on the metaphase I spindle (4/7 eggs) (Figures 4A and 4B), a pattern never seen in *mel-26(RNAi)* alone (0/23 eggs) (Figures 4A and 4B) or in wild-type [7].

To determine whether premature phosphorylation leads to premature degradation, we compared the degradation kinetics of GFP:MEI-1 in wild-type and *egg-3(tm1191)*. In wild-type, GFP:MEI-1 levels remain steady for ~25–30 min after egg exit from the spermatheca (Figures 4C and 4D), consistent with the essential function for MEI-1 during the meiotic divisions, which occur during this time [21]. In contrast, in *egg-3(tm1191)* mutants, GFP:MEI-1 levels started to decline immediately

after spermatheca exit, reaching background levels by 30 min (Figures 4C and 4D). MEI-1 degradation was dependent on MBK-2 as shown by the fact that *egg-3(tm1191);mbk-2(RNAi)* maintained GFP:MEI-1 (Figure S2). We conclude that in the absence of EGG-3, MEI-1 is phosphorylated and degraded prematurely.

EGG-3 Inhibits MBK-2 during Meiosis I

Progression through the meiotic divisions is required for MBK-2 relocalization to the cytoplasm and for timely degradation of MEI-1 and other proteins that require MBK-2 for degradation (e.g., the germ plasm component POS-1) [7, 11]. *mat-1(ax227)* is a temperature-sensitive allele in the CDC-27 subunit of the anaphase-promoting complex/cyclosome (APC/C) [22, 23]. At 25°C, *mat-1(ax227)* eggs are fertilized but arrest in metaphase of meiosis I with GFP:MBK-2 at the cortex (Figure 5A) [7, 11] and GFP:MEI-1 and GFP:POS-1 in the cytoplasm (Figures 5B, 5C, and 5G). To investigate

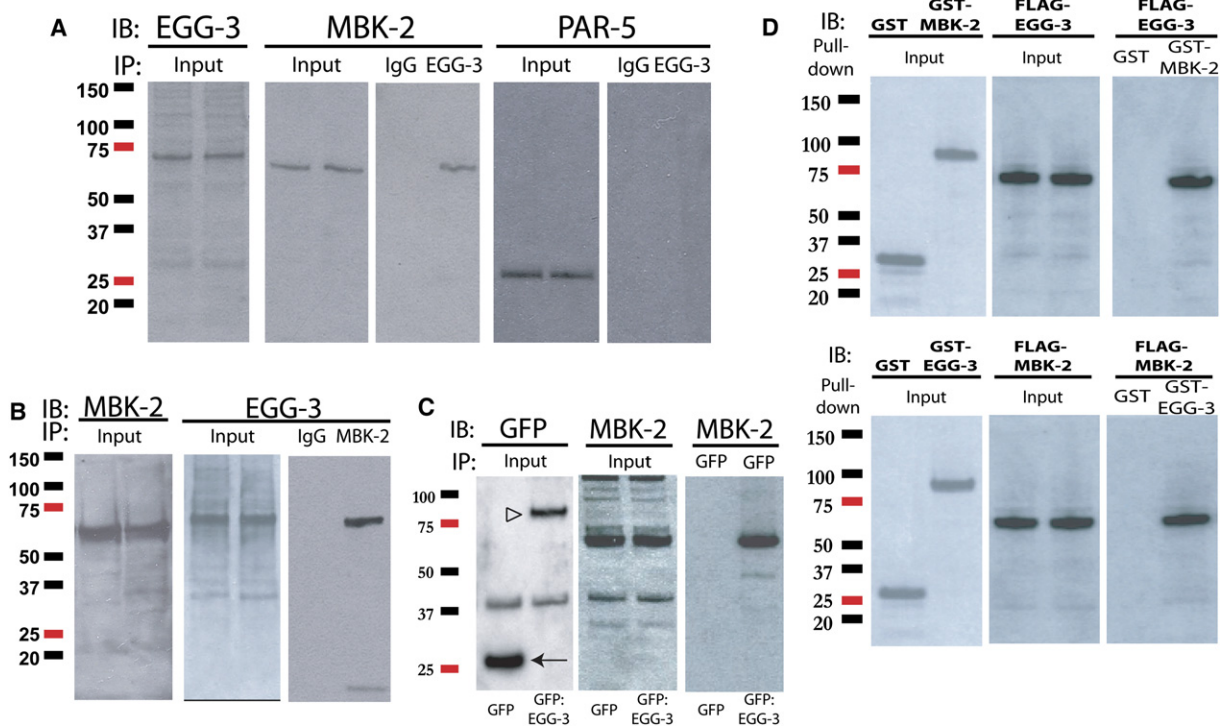


Figure 3. MBK-2 and EGG-3 Form a Complex In Vivo and Interact In Vitro

(A and B) Whole worm extracts (input) were immunoprecipitated (IP) with α -EGG-3 (A) or α -MBK-2 (B) and immunoblotted (IB) with antibodies as indicated. Rabbit IgG was used as a negative control IP antibody. Anti-PAR-5 was used as a negative control target protein in the anti-EGG-3 IP. Input is 1/100th of the IP. Numbers indicate molecular weight markers (kDa). (C) Extracts from worms expressing GFP or GFP:EGG-3 were immunoprecipitated with α -GFP and immunoblotted with antibodies as indicated. Input is 1/100th of the IP. Arrow points to GFP and arrowhead points to GFP:EGG-3. (D) Extracts from *E. coli* expressing FLAG-EGG-3 or FLAG-MBK-2 (input) were pulled down with glutathione-sepharose beads coupled to GST alone, GST-MBK-2, or GST-EGG-3 and immunoblotted with α -FLAG. Input is 1/50th of the pull-down.

whether the lack of MEI-1 and POS-1 degradation is due to sequestration of MBK-2 at the cortex by EGG-3, we inactivated EGG-3 in *mat-1(ax227)* mutants. We found that RNAi depletion of EGG-3 in *mat-1(ax227)* caused (1) GFP:MBK-2 to accumulate in the cytoplasm (Figure 5D) and (2) GFP:MEI-1 and GFP:POS-1 to be degraded in the arrested zygotes (Figures 5E–5G). We conclude that the inability of *mat-1(ax227)* mutants to degrade MEI-1 and POS-1 is due to negative regulation of MBK-2 by EGG-3.

EGG-3 could negatively regulate MBK-2 by inhibiting its intrinsic activity or by limiting its access to substrates. To distinguish between these possibilities, we immunoprecipitated GFP:MBK-2 from wild-type and *mat-1(ax227)* hermaphrodites and assayed for kinase activity against a synthetic peptide (Experimental Procedures). We found that GFP:MBK-2 showed similar activity whether immunoprecipitated from wild-type or *mat-1(ax227)* extracts (Figure 5H). GFP:MBK-2 with a mutation in the ATP binding site (K196R) had only background activity, confirming the specificity of the assay. To verify these results in vivo, we stained *mat-1(ax227);mel-26(RNAi)* zygotes for MEI-1-Ser92P. We observed MEI-1-Ser92P in 36/84 *mat-1(ax227);mel-26(RNAi)* zygotes (Figure 5I). Remarkably, in all positive zygotes, P-MEI-1 was strongest at the cortex. This pattern was dependent on EGG-3: in 29/39 *mat-1(ax227);mel-26(RNAi);egg-3(RNAi)* with positive MEI-1-Ser92P staining, MEI-1-Ser92P was cytoplasmic and showed

no cortical enrichment (Figure 5J). We conclude that EGG-3 restricts active MBK-2 to the cortex during meiosis I.

Cell-Cycle Dependence of GFP:EGG-3 Dynamics

During meiosis II, EGG-3 relocates to subcortical puncta and EGG-3 levels drop such that EGG-3 is not detected after the 2-cell stage (Figures 1, 2, and 6). To investigate whether EGG-3 dynamics depend on meiotic progression, we examined GFP:EGG-3 under conditions where meiotic M phase is blocked in zygotes [*mat-1(RNAi)*] [22] or activated precociously in unfertilized oocytes [*wee-1.3(RNAi)*] [24]. As expected, we found that GFP:EGG-3 remains cortical and stable in *mat-1(RNAi)* zygotes (Figure 6B) and relocates precociously to internal puncta in *wee-1.3(RNAi)* oocytes still in the oviduct (Figure 6C). We conclude that, as for MBK-2, EGG-3 dynamics are stimulated by meiotic progression. Furthermore, EGG-3 degradation depends on the APC/C subunit *mat-1*.

EGG-3 Is a Likely APC/C Target

APC/C is a multisubunit E3 ligase that targets cell-cycle regulators for degradation by the proteasome [25]. Several APC/C recognition motifs have been described, including the destruction or D box (core sequence: RxxL). EGG-3 contains six RxxL motifs (Figure 7A). Mutating each motif revealed that the first two (D boxes 1 and 2)

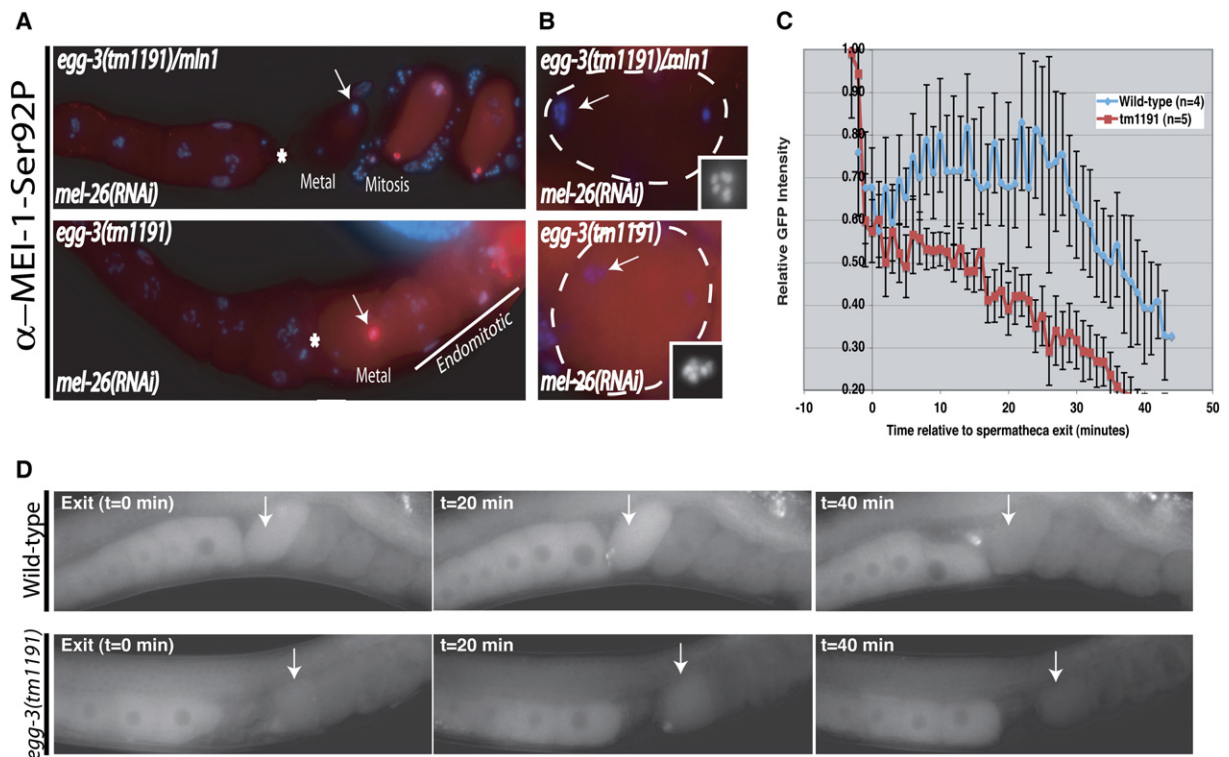


Figure 4. *egg-3* Mutants Phosphorylate and Degrade MEI-1 Prematurely

(A) Dissected gonads fixed and stained with α -MEI-1-Ser92P (red) and DAPI (blue). *mel-26(RNAi)* blocks MEI-1-Ser92P degradation. Arrow marks the meiosis I spindle/chromosome complex. Asterisk marks the spermatheca. Note precocious appearance of MEI-1-Ser92P in metaphase I in the *egg-3* homozygous mutant (bottom). In this example, MEI-1-Ser92P could be detected in both the cytoplasm and on the meiotic spindle.

(B) Metaphase I embryos of the indicated genotypes at higher magnification. Meiotic stage was determined by DAPI staining. Six DAPI-positive bivalents are visible in metaphase I. *egg-3* mutants undergo two meiotic divisions as in wild-type except that they do not extrude polar bodies, resulting in 12 individualized chromosomes visible in metaphase II (see [1], accompanying paper). In this example, MEI-1-Ser92P was predominantly cytoplasmic and was not enriched on the spindle.

(C) GFP:MEI-1 intensity in newly ovulated eggs in wild-type and *egg-3(tm1191)* mutants plotted with respect to minutes since exit from spermatheca. For each time point, GFP:MEI-1 intensity in the ovulated egg was calculated as a fraction of GFP:MEI-1 intensity in an unovulated oocyte in the same hermaphrodite to correct for GFP fluorescence bleaching over time. Note that cytoplasmic GFP:MEI-1 decreases in both wild-type and *egg-3(tm1191)* immediately after ovulation into the spermatheca resulting from accumulation of GFP:MEI-1 on the first meiotic spindle. Error bars represent standard error of measurement (SEM).

(D) Live gonads from wild-type and *egg-3(tm1191)* hermaphrodites expressing GFP:MEI-1. Time is measured relative to spermatheca exit.

are required for degradation (Figures 7B and 7C). Mutations in D boxes 1 and 2 did not disrupt the cortical or puncta localization of GFP:EGG-3 but caused GFP:EGG-3 to persist past the 2-cell stage in the cytoplasm and on the cortex of all blastomeres (Figure 7C). Mutations in other RxxL motifs located within or near the PTP domain blocked GFP:EGG-3's ability to localize to the cortex but did not affect degradation (Figure 7B), indicating that localization to the cortex is not a prerequisite for degradation. Western analysis confirmed that all fusion proteins were expressed at similar levels (Figure 7D), ruling out overexpression as a possible cause for the degradation defects. EGG-3 degradation was also blocked when the proteasome subunit *rpn-7* was partially inactivated by RNAi (75% of *rpn-7(RNAi)* hermaphrodites [n = 35] had 2-cell or older embryos with cortical EGG-3) (Figure 7C). We conclude that EGG-3 is likely to be targeted for degradation by APC/C and to be degraded by the proteasome.

If EGG-3 degradation were the only factor contributing to MBK-2 release in the cytoplasm, GFP:MBK-2 should

also localize to cell cortices in *rpn-7(RNAi)* embryos. In contrast, we found that GFP:MBK-2 remained cytoplasmic in most *rpn-7(RNAi)* embryos (Figure 7C). Cortical GFP:MBK-2 was not detected in 4-cell and older embryos in 95% of hermaphrodites examined (n = 49). In the remaining 5% of hermaphrodites examined, faint cortical GFP:MBK-2 was observed in one or more embryos (data not shown). We conclude that, although EGG-3 degradation may contribute to MBK-2 release, it may not be the only factor involved.

Discussion

In this study, we report that the cortical protein EGG-3 is required for MBK-2 localization to the cortex. We demonstrate that (1) EGG-3 forms a complex with MBK-2 in vivo and in vitro, (2) EGG-3 functions as a negative regulator of MBK-2 during meiosis I, and (3) EGG-3 is degraded during the meiotic divisions in an APC/C- and proteasome-dependent manner. We discuss the

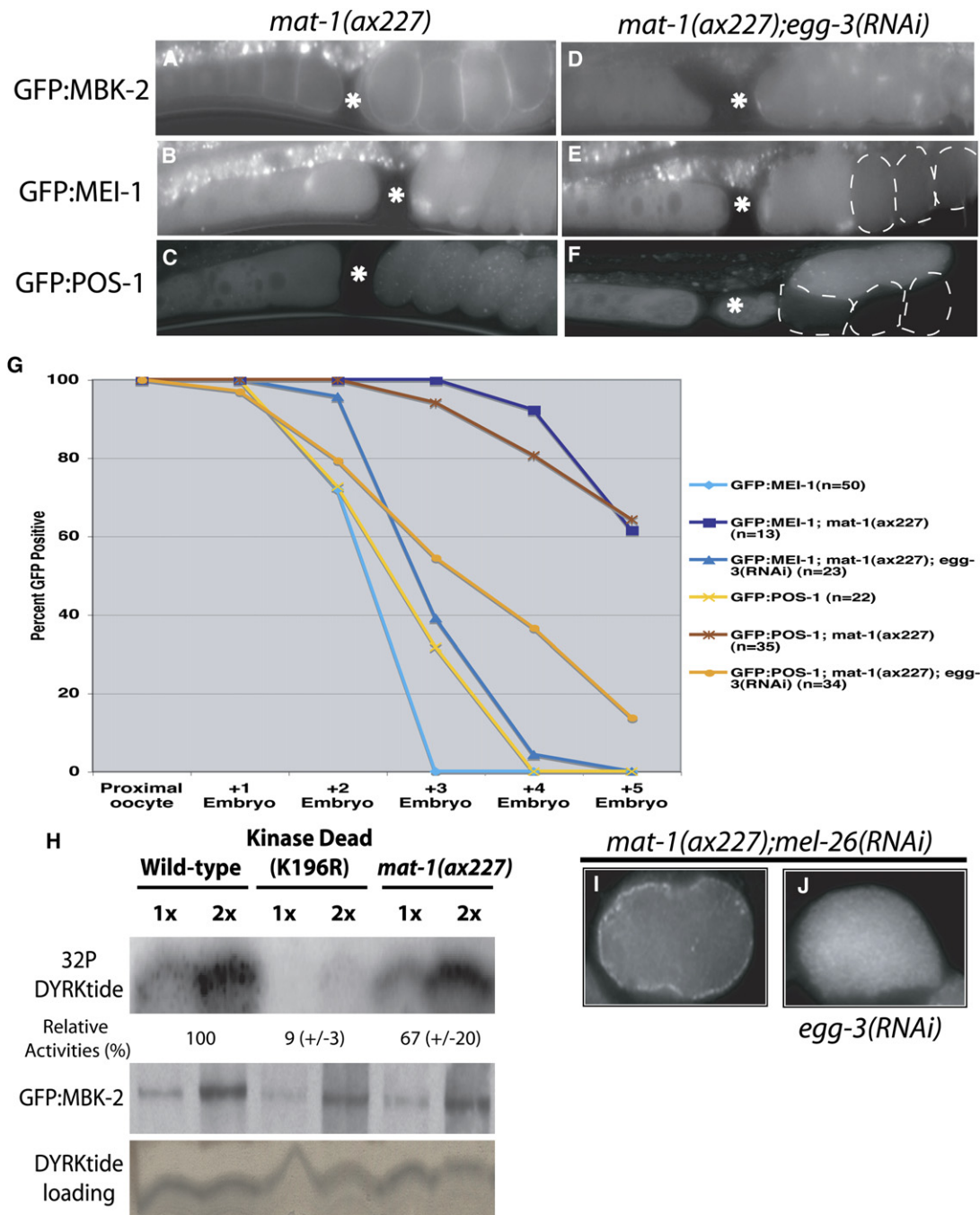


Figure 5. Loss of *egg-3* Suppresses the Degradation Defect of *mat-1* Zygotes by Releasing Active MBK-2 from the Cortex

(A–F) Gonads of live *mat-1(ax227)* (A–C) or *mat-1(ax227);egg-3(RNAi)* (D–F) hermaphrodites expressing GFP:MBK-2 (A, D), GFP:MEI-1 (B, E), or GFP:POS-1 (C, F). Asterisk denotes the position of the spermatheca; dashed circles mark embryos with lower GFP levels. Gut autofluorescence is visible above oocytes and embryos.

(G) Percent of embryos positive for GFP:MEI-1 or GFP:POS-1 were plotted with respect to position in the uterus of wild-type, *mat-1(ax227)*, and *mat-1(ax227);egg-3(RNAi)* hermaphrodites. Ovulation rates were not significantly different between these genotypes (Figure S3).

(H) Kinase assay comparing the kinase activity of GFP:MBK-2 immunoprecipitated from wild-type or *mat-1(ax227)* worms against a synthetic peptide (DYRKtide). GFP:MBK-2(K196R) has a mutation in the ATP binding site and is inactive [7]. Loading of GFP:MBK-2 was determined by immunoblotting with GFP antibody and loading of DYRKtide by Silver Quest staining (Invitrogen). ³²P incorporation was detected with a Phosphorimager (Amersham). Numbers represent average percent activity with respect to wild-type ± standard deviation from three independent experiments.

(I and J) Fixed zygotes from *mat-1(ax227);mel-26(RNAi)* with (J) or without (I) *egg-3(RNAi)* and stained with α-MEI-1-Ser92P. Note the cortical accumulation in *mat-1(ax227);mel-26(RNAi)*.

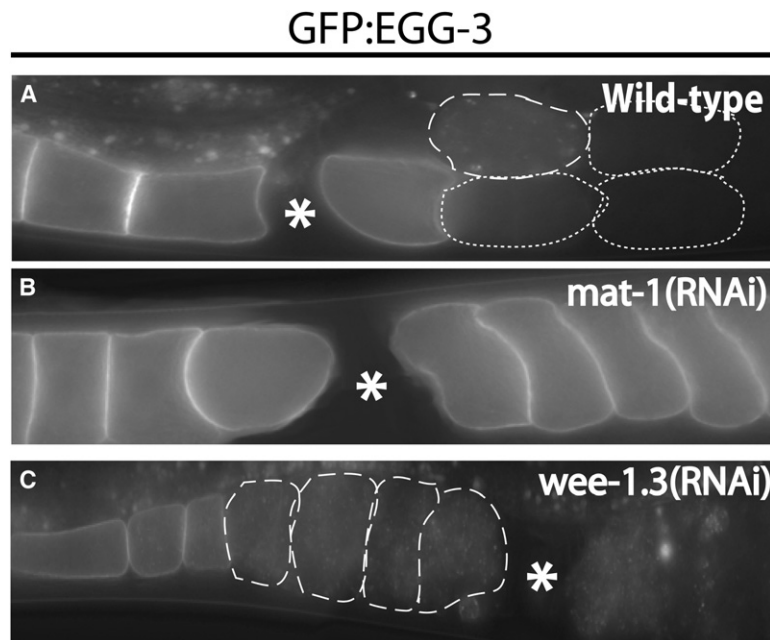


Figure 6. GFP:EGG-3 Internalization and Degradation Is Controlled by the Meiotic Cell Cycle

Live wild-type (A), *mat-1(RNAi)* (B), or *wee-1.3(RNAi)* (C) hermaphrodites expressing GFP:EGG-3. Eggs with GFP:EGG-3 in cytoplasmic puncta are outlined with a dashed line, and eggs with no GFP:EGG-3 are outlined with a dotted line.

implications of these findings in the context of the oocyte-to-zygote transition.

Cortical Tethering as a Mechanism to Restrict MBK-2 from Its Cytoplasmic Substrates

EGG-3 contains a predicted protein-tyrosine phosphatase (PTP) domain missing certain active site residues (see [1], accompanying paper in this issue). PTPs with similar “natural mutations” have been shown to lack phosphatase activity, although some retain the ability to bind to phosphorylated substrates [17, 18]. We have shown that EGG-3 and MBK-2 exist in a complex in vivo and interact directly in vitro. Because MBK-2 is predicted to autophosphorylate on tyrosines, an attractive possibility is that EGG-3 recognizes a phosphorylated tyrosine in MBK-2. EGG-3, however, also interacts with kinase-dead MBK-2 synthesized in *E. coli*, which is predicted not to contain any phosphorylated tyrosines (K.C.-C.C., unpublished data). Although EGG-3 and MBK-2 interact directly in vitro, this interaction may not be sufficient to localize MBK-2 to the cortex in vivo, because cortical EGG-3 is not sufficient to recruit MBK-2 when stabilized in 2-cell and older embryos. Consistent with this view, we identified two other genes in our screen required for MBK-2 localization to the cortex. Depletion of these genes by RNAi does not affect EGG-3 localization to the cortex (K.C.-C.C., unpublished data), suggesting that these genes are required, in addition to EGG-3, to anchor MBK-2.

Several lines of evidence support the hypothesis that cortical anchoring limits MBK-2's ability to phosphorylate cytoplasmic targets during meiosis I. First, in wild-type embryos, appearance of MEI-1-S92P during meiosis II correlates with relocalization of GFP:MBK-2 from the cortex to the cytoplasm [7]. Second, in *egg-3* mutants, MBK-2 is constitutively cytoplasmic and MEI-1 is phosphorylated prematurely in meiosis I (as observed in *egg-3(tm1191)*; *mel-26(RNAi)*; this work). Third, in *mat-1* mutants arrested in meiosis I, GFP:MBK-2

remains cortical and degradation of GFP:MEI-1 and GFP:POS-1 is blocked [7, 11]. Fourth, the *mat-1* block can be reversed by eliminating EGG-3 and forcing MBK-2 to the cytoplasm (this work).

Cortical tethering of MBK-2 during meiosis I could inhibit MBK-2 activity directly or indirectly, by reducing access to cytoplasmic targets. We favor the latter because GFP:MBK-2 immunoprecipitated from *mat-1* mutants is active and because some MEI-1-S92P can be detected at the cortex in *mat-1(ts)*; *mel-26(RNAi)* zygotes. One possibility is that the cortex functions as a diffusion barrier between MBK-2 and the bulk of its cytoplasmic targets.

Cell-Cycle Regulation of MBK-2

What releases MBK-2 from the cortex? Starting in anaphase of meiosis I, EGG-3 and GFP:MBK-2 localize to subcortical puncta that invade the cytoplasm during the second meiotic division. Similar structures have been observed with a GFP fusion to the membrane protein caveolin [26], raising the possibility that EGG-3/MBK-2 are internalized on the surface of endocytosed vesicles. During internalization, total EGG-3 levels decrease and cytoplasmic MBK-2 levels increase. The dynamics of EGG-3 degradation resemble those described for GFP:cyclin B1 [10], a known target of the anaphase-promoting complex/cyclosome (APC/C) in yeast and vertebrates [25]. Consistent with being an APC/C target, EGG-3 degradation depends on two D boxes, the APC/C subunit *mat-1*, and the proteasome. We suggest that APC/C-dependent degradation of EGG-3 is one of the mechanisms by which the meiotic cell cycle activates MBK-2. In fact, the finding that the MEI-1 and POS-1 degradation defects of *mat-1* mutants can be suppressed by depleting *egg-3* suggests that APC/C's only essential role in activating MBK-2 is to antagonize EGG-3.

Stabilization of EGG-3 is not sufficient to recruit MBK-2 back to the cortex after the zygote stage, suggesting

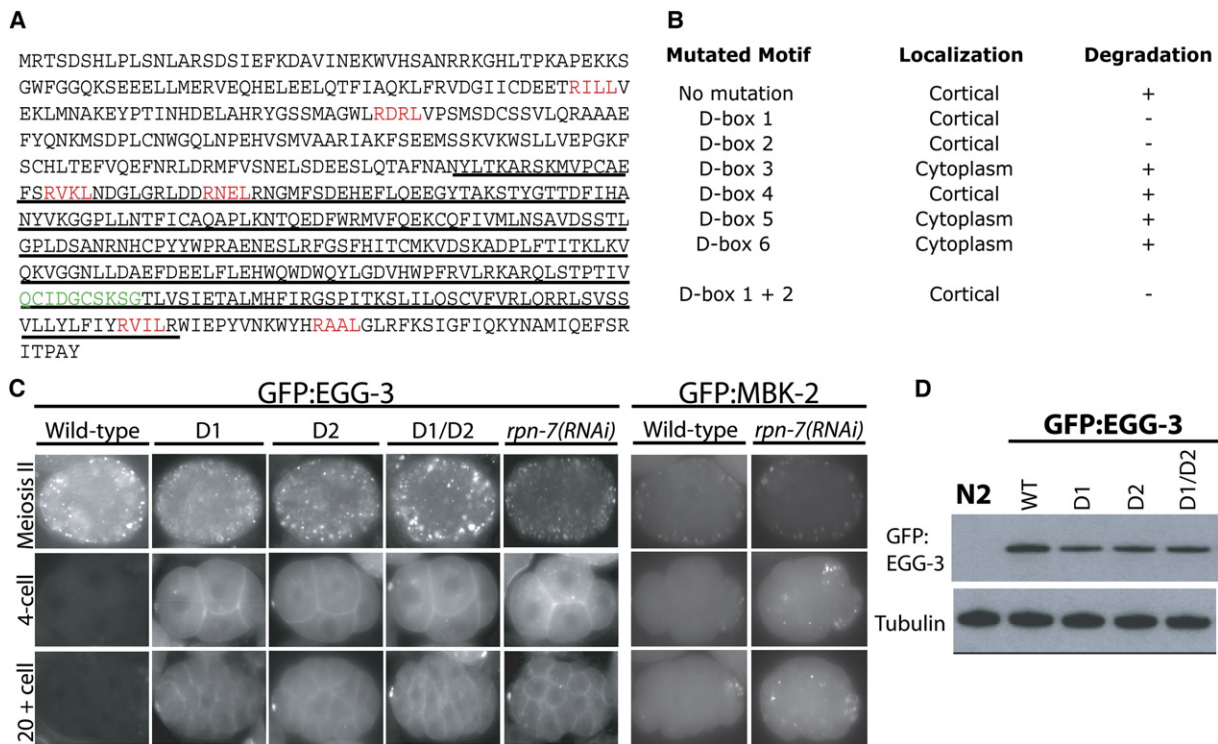


Figure 7. EGG-3 Is a Likely Target of the Anaphase-Promoting Complex/Cyclosome

(A) Amino acid sequence of EGG-3. PTP domain is underlined, D boxes are marked in red, and the phosphatase active site is green.
 (B) List of mutants tested for effect on cortical localization and degradation of GFP:EGG-3.
 (C) Images of live embryos expressing GFP fusions as indicated.
 (D) Western showing similar expression levels of the wild-type and mutant GFP:EGG-3 fusions. The increased stability of some of the fusions, as shown in (C), does not result in detectably higher levels in the western, possibly because the increase in 2-cell and later stages is modest compared to total EGG-3 present in oocytes and early zygotes.

that progression through the meiotic divisions also suppresses the activity of other factors required for MBK-2 cortical localization. One possibility is that endocytosis during the meiotic divisions removes several factors at once from the cortex required for MBK-2 anchoring.

In *egg-3;mel-26* mutants, MEI-1-S92P appears prematurely in eggs that have progressed to metaphase I, but is not observed in oocytes that have not yet been ovulated. EGG-3-independent mechanisms must therefore operate in those earlier stages to keep MBK-2 inactive. We propose that MBK-2 activation occurs in two steps: (1) activation of kinase activity during ovulation and/or the first meiotic division by an unknown mechanism, and (2) release of active MBK-2 from the cortex during the second meiotic division via APC/C-dependent internalization and degradation of EGG-3 (and possibly other factors).

Spatial Regulation: A Common Way to Regulate Kinases in Oocytes?

The transition from oocyte to zygote occurs in the absence of mRNA transcription and thus must rely on post-transcriptional mechanisms to change gene activity. Our studies with MBK-2 illustrate the role of spatial compartmentalization as an efficient mechanism to keep an active kinase away from the bulk of its targets until the right time. A similar mechanism has recently been implicated in the downregulation of protein kinase A (PKA) in mouse oocytes [27]. PKA maintains prophase

arrest in oocytes before maturation. During maturation, the PKA catalytic subunit α relocalizes from the cortex to the cytoplasm, and the regulatory subunit β relocalizes from the cortex/cytoplasm to mitochondria [28, 29]. Elimination of the anchor protein AKAP1 prevents β relocalization to mitochondria and blocks oocyte maturation, apparently because of excess PKA remaining at the cortex [29]. These observations have led to a model whereby active PKA is downregulated during maturation by AKAP1, which sequesters the β subunit away from cortical targets [27]. The mechanisms that induce β relocalization are not known but have been proposed to be linked to entry into meiotic M phase [29]. We suggest that internalization of cortical proteins stimulated by the advancing cell cycle simultaneously “inactivates” and “activates” different sets of kinases by removing them from (e.g., PKA) or releasing them to (e.g., MBK-2) their substrates. This reorganization changes the global landscape of kinase/substrate interactions and irreversibly commits the oocyte to maturation and preparation for embryogenesis.

The EGG-3/MBK-2 Complex Links the Events of Oocyte Maturation and Egg Activation

In addition to its role in regulating MBK-2 described here, EGG-3 also functions in egg activation. *egg-3* oocytes undergo maturation, meiosis, and fertilization but do not form polar bodies or an egg shell, two processes dependent on fertilization (see [1], accompanying paper in this

issue). In contrast, *mbk-2* mutants undergo egg activation, but fail to degrade MEI-1, OMA-1, and germ plasm proteins, processes dependent on oocyte maturation [7]. The finding that MBK-2 and EGG-3 exist in a complex suggests an intimate connection between the egg remodeling events triggered by oocyte maturation and those triggered by egg activation. A cortical complex with the ability to respond to both the advancing cell cycle and to fertilization may help orchestrate the proper timing of the many aspects of the oocyte-to-zygote transition, coordinating loss of germ cell fate with acquisition of zygotic totipotency. A challenge for the future will be to understand how cell cycle- and fertilization-dependent signals converge on the EGG-3/MBK-2 complex. Our finding that the egg activation protein EGG-3 is a negative regulator of MBK-2 that is degraded in an APC/C-dependent manner offers a first insight into this process.

Experimental Procedures

Nematode Strains and Temperature Shift Experiments

C. elegans strains (Table S1) were derived from the wild-type Bristol strain N2 and reared by standard procedures [30]. *egg-3(tm1191)* was a gift from S. Mitani (Tokyo Women's Medical College, National Bioresource Project of Japan) and is a 480 bp deletion predicted to result in a termination codon at amino acid 160. *tm1191/tm1191* hermaphrodites do not stain with anti-EGG-3 serum raised against amino acids 29–49 (see below), confirming that *tm1191* is a null. *mat-1(ax227)* hermaphrodites were maintained at 16°C and shifted to 25°C as L4 larvae.

Transgene Construction and Transformation

All transgenes in this study were driven by the *pie-1* promoter and 3'UTR for maternal expression [31]. GFP:MBK-2 is described in [11] and rescues the *mbk-2* null allele (*pk1427*). The *egg-3* ORF was amplified from cDNA and cloned into pID3.01 [31] to create GFP:EGG-3. D box mutations were generated with QuickChange site-directed mutagenesis kit (Stratagene) and confirmed by sequencing. Isoform C of MBK-2 was amplified from genomic DNA and cloned into pID2.02 [31] to create MBK-2:6XHis. Microparticle bombardment [32] was used to generate several independent lines for each transgene, and a single representative line was selected for further experiments.

RNAi

Feeding clones corresponding to predicted kinases and phosphatases (WORMBASE) were cherry-picked from the Ahringer feeding library [33], grown in LB + ampicillin (100 µg/ml) at 37°C, and spread on NNGM (nematode nutritional growth medium) + Amp (100 µg/ml) + IPTG (80 µg/ml). ~30 GFP:MBK-2 L2 worms were incubated on the plates for 48 hr at 25°C before screening with a fluorescence compound microscope.

For individual RNAi experiments, L4 hermaphrodites were fed at 25°C for 24–27 hr before examination, except for *rpn-7(RNAi)*, which were examined after 16 hr of feeding.

Antibodies

Anti-MBK-2 sera were generated against the N-terminal peptide CMHSKIPKSPSNES in rabbit (Bethyl Laboratories; used for immunofluorescence) and against recombinant GST:MBK-2 in rabbit (Covance; used for western). Anti-EGG-3 serum was generated against N-terminal peptide KVVHSANRRKGLTPKAPEKK in guinea pig (Covance). EGG-3 and MBK-2 antibodies blotted against whole worm extracts identified a prominent band migrating in the expected size range (Figure 3). Immunofluorescence experiments comparing staining in wild-type and null mutants confirmed specificity (Figure S1).

Worm Extract Preparation

Adult hermaphrodites suspended in ice-cold lysis/homogenization buffer (50 mM HEPES [pH 7.4], 300 mM KCl, 1 mM MgCl₂, 1 mM

EGTA, 10% glycerol, 0.5 mM DTT, 0.05% NP-40, and Complete Mini protease inhibitor tablet [Roche]) were lysed by three freeze-thaw cycles in liquid nitrogen and vortexing with glass beads (Sigma) or by grinding with a mortar and pestle. Extracts were centrifuged at 4°C, 14,000 rpm for 15 min and 30 min, frozen in liquid nitrogen, and stored at –80°C.

Immunoprecipitations and Western Blotting

Extracts were precleared with protein A-agarose beads coupled to 60 µl of rabbit IgG (1 mg/ml, Sigma) or 10 µl of guinea pig IgG (Sigma). GFP, MBK-2, and EGG-3 antibodies were coupled to protein A magnetic beads (NEB) (GFP) or protein A-agarose (Pierce) (MBK-2, EGG-3). Beads were incubated with precleared extracts at 4°C overnight and washed three times with ice-cold homogenization buffer. Precipitates and input were run on a 4%–12% SDS-PAGE (Invitrogen). The following antibodies (and dilutions) were used in western blotting: anti-MBK-2 (1:2500), anti-EGG-3 (1:5000), anti-PAR-5 (1:500, gift from A. Golden), anti-GFP (JL-8, 1:1000; BD Biosciences), anti-FLAG M2 (1:4000, Sigma), anti-GST (1:200, Santa Cruz), anti-tubulin (E7, 1:1000, Developmental Studies Hybridoma Bank), HRP-conjugated anti-rabbit (1:10,000, Pharmacia), anti-mouse (1:10,000, Amersham Pharmacia), and anti-guinea pig (1:10,000, Sigma).

DYRKtide Kinase Assay

Kinase assays were performed as described in [34]. GFP:MBK-2 immunoprecipitates were incubated with DYRKtide/Woodtide (KKISGRLSPIMTEQ, 50 µM final concentration UBI) in kinase buffer (10 mM MgCl₂, 50 mM Tris-HCl [pH 7.5], 0.1 mM EGTA, 0.1% beta-mercaptoethanol [BME]) with [³²P]ATP (Amersham Pharmacia) for 10 min at 30°C. Reactions were stopped with 1× NuPage LDS Sample Buffer (Invitrogen) and BME (5% v/v). Samples were boiled for 5 min, beads removed with a magnet, and supernatants were separated on a 16% Tricine gel (Invitrogen). DYRKtide was visualized with the SilverQuest silver staining kit (Invitrogen). ³²P incorporation was detected in the same gel by Phosphorimager (Amersham Pharmacia).

Percent activity (Figure 5H) was calculated by measuring ³²P incorporation with ImageQuant 5.2 (Molecular Dynamics) normalized for the amount of immunoprecipitated GFP:MBK-2 as measured by western (ImageJ gel tools) and expressed as percent of wild-type activity.

GST Pull-Down Assay

mbk-2 and *egg-3* ORFs were amplified from cDNA, cloned into pDEST-15 (GST fusions) or pKC5.02 (FLAG fusions) to create amino-terminal fusions, and expressed in BL21(DE3) gold (Invitrogen). Glutathione-Sepharose 4B beads (Amersham Pharmacia) were incubated with GST extracts at 4°C for 2 hr in PBST (phosphate-buffered saline with 1% Triton X-100), washed, incubated with crude FLAG extracts in binding buffer (20 mM HEPES [pH 7.6], 200 mM NaCl, 1 mM EDTA, 6% glycerol, 0.5 mM DTT, 0.1% NP-40, and Complete Mini protease inhibitor tablet [Roche]) at 4°C for 2 hr, and washed. The bound proteins were eluted by boiling in 2× LDS sample buffer (Invitrogen) and subjected to 4%–12% SDS-PAGE (Invitrogen) for western blot analysis.

Immunofluorescence, Microscopy, and Quantification

Embryos were prepared as in [7]. Primary antibodies used were mouse monoclonal anti-GFP (3E6, 1:100; Molecular Probes), rabbit anti-MBK-2 (1:10,000, Bethyl Laboratories), guinea pig anti-EGG-3 (1:10,000), rabbit anti-MEI-1-Ser92P (1:2000) [7], and mouse anti-His (1:10,000; Sigma). Secondary antibodies were Cy3 goat anti-mouse (1:200, Jackson ImmunoResearch), Alexa 568 goat anti-rabbit (1:250, Molecular Probes), and Alexa 488/Alexa 568 goat anti-guinea pig (1:200, Molecular Probes). Images were acquired with a Hamamatsu ORCA-ER digital camera attached to a Zeiss Axioplan 2, processed with IPLab software (Scanalytics, Inc.) and Photoshop CS. Values in Figure 2E were obtained by measuring pixel intensity (background subtracted) in a 50 × 50 pixel square within the embryo (cytoplasmic GFP:MBK-2) or a 720 × 520 pixel rectangle surrounding the total embryo (total GFP:MBK-2 and total EGG-3) for a minimum of 3 fixed embryos from each stage. Values were normalized such that the maximum intensity for each series equals 1. Values in Figure 4C were obtained from time-lapse images by computing average GFP fluorescence for three 25-pixel squares placed on (1) a preovulation

oocyte, (2) a newly ovulated egg, and (3) a 2-cell or older embryo (background), avoiding spindle and nuclei. For each time point, background was subtracted and GFP:MEI-1 intensity in the newly ovulated egg was expressed as a fraction of GFP:MEI-1 in the nonovulated egg (to correct for bleaching during the course of the experiment).

Supplemental Data

Three figures and one table are available at <http://www.current-biology.com/cgi/content/full/17/18/1545/DC1/>.

Acknowledgments

We thank R. Maruyama and A. Singson for sharing unpublished results and for comments on the manuscript, and S. Mitani and the National Bioresource Project of Japan for *egg-3(tm1191)*. This work was supported by NIH grant HD37047. G.S. is an investigator of the Howard Hughes Medical Institute.

Received: July 12, 2007

Revised: August 2, 2007

Accepted: August 3, 2007

Published online: September 13, 2007

References

1. Maruyama, R., Velarde, N.V., Klancer, R., Gordon, S., Kandanale, P., Parry, J.M., Hang, J.S., Rubin, J., Stewart-Michaelis, A., Schweinsberg, P., et al. (2007). EGG-3 regulates cell-surface and cortex rearrangements during egg activation in *Caenorhabditis elegans*. *Curr. Biol.* **17**, 1555–1560.
2. Stitzel, M.L., and Seydoux, G. (2007). Regulation of the oocyte-to-zygote transition. *Science* **316**, 407–408.
3. Kishimoto, T. (2003). Cell-cycle control during meiotic maturation. *Curr. Opin. Cell Biol.* **15**, 654–663.
4. Malcuit, C., Kurokawa, M., and Fissore, R.A. (2006). Calcium oscillations and mammalian egg activation. *J. Cell. Physiol.* **206**, 565–573.
5. Voronina, E., and Wessel, G.M. (2003). The regulation of oocyte maturation. *Curr. Top. Dev. Biol.* **58**, 53–110.
6. Su, Y.Q., Sugiura, K., Woo, Y., Wigglesworth, K., Kamdar, S., Af-fourtit, J., and Eppig, J.J. (2007). Selective degradation of transcripts during meiotic maturation of mouse oocytes. *Dev. Biol.* **302**, 104–117.
7. Stitzel, M.L., Pellettieri, J., and Seydoux, G. (2006). The *C. elegans* DYRK kinase MBK-2 marks oocyte proteins for degradation in response to meiotic maturation. *Curr. Biol.* **16**, 56–62.
8. Walker, A.K., Boag, P.R., and Blackwell, T.K. (2007). Transcription reactivation steps stimulated by oocyte maturation in *C. elegans*. *Dev. Biol.* **304**, 382–393.
9. Yamamoto, I., Kosinski, M.E., and Greenstein, D. (2006). Start me up: cell signaling and the journey from oocyte to embryo in *C. elegans*. *Dev. Dyn.* **235**, 571–585.
10. McNally, K.L., and McNally, F.J. (2005). Fertilization initiates the transition from anaphase I to metaphase II during female meiosis in *C. elegans*. *Dev. Biol.* **282**, 218–230.
11. Pellettieri, J., Reinke, V., Kim, S.K., and Seydoux, G. (2003). Coordinate activation of maternal protein degradation during the egg-to-embryo transition in *C. elegans*. *Dev. Cell* **5**, 451–462.
12. Quintin, S., Mains, P.E., Zinke, A., and Hyman, A.A. (2003). The MBK-2 kinase is required for inactivation of MEI-1/katanin in the one-cell *Caenorhabditis elegans* embryo. *EMBO Rep.* **4**, 1175–1181.
13. Pang, K.M., Ishidate, T., Nakamura, K., Shirayama, M., Trzepak, C., Schubert, C.M., Priess, J.R., and Mello, C.C. (2004). The mini-brain kinase homolog, *mbk-2*, is required for spindle positioning and asymmetric cell division in early *C. elegans* embryos. *Dev. Biol.* **265**, 127–139.
14. Becker, W., and Joost, H.G. (1999). Structural and functional characteristics of Dyrk, a novel subfamily of protein kinases with dual specificity. *Prog. Nucleic Acid Res. Mol. Biol.* **62**, 1–17.
15. Nishi, Y., and Lin, R. (2005). DYRK2 and GSK-3 phosphorylate and promote the timely degradation of OMA-1, a key regulator of the oocyte-to-embryo transition in *C. elegans*. *Dev. Biol.* **288**, 139–149.
16. Shirayama, M., Soto, M.C., Ishidate, T., Kim, S., Nakamura, K., Bei, Y., van den Heuvel, S., and Mello, C.C. (2006). The conserved kinases CDK-1, GSK-3, KIN-19, and MBK-2 promote OMA-1 destruction to regulate the oocyte-to-embryo transition in *C. elegans*. *Curr. Biol.* **16**, 47–55.
17. Hunter, T. (1998). Anti-phosphatases take the stage. *Nat. Genet.* **18**, 303–305.
18. Wishart, M.J., and Dixon, J.E. (1998). Gathering STYX: phosphatase-like form predicts functions for unique protein-interaction domains. *Trends Biochem. Sci.* **23**, 301–306.
19. Morton, D.G., Shakes, D.C., Nugent, S., Dichoso, D., Wang, W., Golden, A., and Kempfues, K.J. (2002). The *Caenorhabditis elegans par-5* gene encodes a 14-3-3 protein required for cellular asymmetry in the early embryo. *Dev. Biol.* **241**, 47–58.
20. Pintard, L., Willis, J.H., Willems, A., Johnson, J.L., Srayko, M., Kurz, T., Glaser, S., Mains, P.E., Tyers, M., Bowerman, B., et al. (2003). The BTB protein MEL-26 is a substrate-specific adaptor of the CUL-3 ubiquitin-ligase. *Nature* **425**, 311–316.
21. Srayko, M., Buster, D.W., Bazirgan, O.A., McNally, F.J., and Mains, P.E. (2000). MEI-1/MEI-2 katanin-like microtubule severing activity is required for *Caenorhabditis elegans* meiosis. *Genes Dev.* **14**, 1072–1084.
22. Golden, A., Sadler, P.L., Wallenfang, M.R., Schumacher, J.M., Hamill, D.R., Bates, G., Bowerman, B., Seydoux, G., and Shakes, D.C. (2000). Metaphase to anaphase (*mat*) transition-defective mutants in *Caenorhabditis elegans*. *J. Cell Biol.* **151**, 1469–1482.
23. Shakes, D.C., Sadler, P.L., Schumacher, J.M., Abdolrasulnia, M., and Golden, A. (2003). Developmental defects observed in hypomorphic anaphase-promoting complex mutants are linked to cell cycle abnormalities. *Development* **130**, 1605–1620.
24. Burrows, A.E., Scurman, B.K., Kosinski, M.E., Richie, C.T., Sadler, P.L., Schumacher, J.M., and Golden, A. (2006). The *C. elegans* Myt1 ortholog is required for the proper timing of oocyte maturation. *Development* **133**, 697–709.
25. Thornton, B.R., and Toczyski, D.P. (2006). Precise destruction: an emerging picture of the APC. *Genes Dev.* **20**, 3069–3078.
26. Sato, K., Sato, M., Audhya, A., Oegema, K., Schweinsberg, P., and Grant, B.D. (2006). Dynamic regulation of caveolin-1 trafficking in the germ line and embryo of *Caenorhabditis elegans*. *Mol. Biol. Cell* **17**, 3085–3094.
27. Burton, K.A., and McKnight, G.S. (2007). PKA, germ cells, and fertility. *Physiology (Bethesda)* **22**, 40–46.
28. Brown, R.L., Ord, T., Moss, S.B., and Williams, C.J. (2002). A-kinase anchor proteins as potential regulators of protein kinase A function in oocytes. *Biol. Reprod.* **67**, 981–987.
29. Newhall, K.J., Criniti, A.R., Cheah, C.S., Smith, K.C., Kafer, K.E., Burkart, A.D., and McKnight, G.S. (2006). Dynamic anchoring of PKA is essential during oocyte maturation. *Curr. Biol.* **16**, 321–327.
30. Brenner, S. (1974). The genetics of *Caenorhabditis elegans*. *Genetics* **77**, 71–94.
31. D'Agostino, I., Merritt, C., Chen, P.L., Seydoux, G., and Subramaniam, K. (2006). Translational repression restricts expression of the *C. elegans* Nanos homolog NOS-2 to the embryonic germline. *Dev. Biol.* **292**, 244–252.
32. Praitis, V., Casey, E., Collar, D., and Austin, J. (2001). Creation of low-copy integrated transgenic lines in *Caenorhabditis elegans*. *Genetics* **157**, 1217–1226.
33. Kamath, R.S., Fraser, A.G., Dong, Y., Poulin, G., Durbin, R., Gotta, M., Kanapin, A., Le Bot, N., Moreno, S., Sohrmann, M., et al. (2003). Systematic functional analysis of the *Caenorhabditis elegans* genome using RNAi. *Nature* **421**, 231–237.
34. Lochhead, P.A., Sibbet, G., Kinstrie, R., Cleghon, T., Ryllatt, M., Morrison, D.K., and Cleghon, V. (2003). dDYRK2: a novel dual-specificity tyrosine-phosphorylation-regulated kinase in *Drosophila*. *Biochem. J.* **374**, 381–391.